Pedosphere **36**(2): 603–613, 2026
doi: 10.1016/j.pedsph.2024.12.001
ISSN 1002-0160/CN 32-1315/P

Published by Elsevier B.V. and Science Press

PEDOSPHERE

www.elsevier.com/locate/pedosphere

Effects of soil erosion-deposition rate and mollic epipedon thickness on sloping farmland soil nutrients in the Mollisol region of Northeast China

Chang LIU[1], Gang LIU[1,2,*], Qiong ZHANG[1,2], Chenxi DAN[1], Yuqian HAN[1], Enshuai SHEN[1] and Zhen GUO[3]

[1]*State Key Laboratory of Soil and Water Conservation and Desertification Control, College of Soil and Water Conservation Science and Engineering (Institute of Soil and Water Conservation), Northwest A&F University, Yangling 712100 (China)*
[2]*Institute of Soil and Water Conservation, Chinese Academy of Sciences and Ministry of Water Resources, Yangling 712100 (China)*
[3]*Sichuan Huabiaoce Testing Technology Co., Ltd., Chengdu 610097 (China)*

(Revised August 26, 2024; revised October 20, 2024; accepted November 25, 2024)

ABSTRACT

Severe soil erosion in Northeast China has led to significant declines in the mollic epipedon thickness (MET) and soil nutrient contents (SNs), thereby reducing soil productivity. However, the correlations among MET, soil erosion-deposition rate (SED), and SNs remain uncertain. This study aimed to explore the combined effects of SED and MET on SNs. Three sloping farmlands in Keshan, Binxian, and Hailun, Heilongjiang in the Mollisol region of Northeast China were selected to investigate the distribution characteristics of MET, SED, and SNs. The slope lengths and gradients were 200–276 m and 1.3°–1.9°, respectively. An inverse correlation was observed between SED and MET. The SNs were lower in the middle section of the slope, whereas they increased in the foot section. The changes in SED, MET, and SNs exhibited a wave-like trend. According to correlation analysis, SED was negatively correlated to SNs, while MET was positively correlated with SNs. However, when MET exceeded 40 cm, the inverse relationship between SED and SNs diminished. Consequently, MET cannot be disregarded in the prevention and control of soil erosion. A regression equation was fitted to model the relationship between MET (less than 40 cm) and SNs and SED. Comprehensive consideration of SED, MET, and SNs at different positions on the slopes is particularly crucial when designing effective soil and water conservation measures. This study provides a scientific basis for the control of soil erosion and the protection of Mollisol resources.

Key Words: black soil, crop yield, ^{137}Cs-tracing technology, ground penetrating radar, quantitative relationship, soil fertility

Citation: Liu C, Liu G, Zhang Q, Dan C X, Han Y Q, Shen E S, Guo Z. 2026. Effects of soil erosion-deposition rate and mollic epipedon thickness on sloping farmland soil nutrients in the Mollisol region of Northeast China. *Pedosphere*. **36**(2): 603–613.

INTRODUCTION

The Mollisol region in Northeast China, which constitutes a significant national grain production center, contributed 21% of the national total grain production in 2022 (IGSNRR CAS, 2023). However, due to more than a century of agricultural production, accompanied by frequent rainstorms, fierce winds, annual freeze-thaw circulation, and increasing human activities, soil erosion has markedly increased in this region (Zhang *et al*., 2007; Liu *et al*., 2011). The first national water resource survey and the Special Plan for Erosion Gully Control in Northeast China's Black Soil Region (2016–2030) indicate that there are 291 700 eroding gullies in the region, with 58.06% distributed on cultivated land (Zhang, 2020). In Mollisol region of Northeast China, the mollic epipedon thickness (MET) has declined by 0.32 cm year^{-1} on average over the past 40 years (Liu *et al*., 2022), which seriously threatens crop production. Feng *et al*. (2018) found that crop yields sharply declined when MET was less than 20 cm. Hence, maintaining a sufficient MET is crucial for sustainable agricultural productivity.

Soil nutrients play a vital role in supporting plant development and influencing agricultural productivity (Adimassu *et al*., 2014). The interplay between soil erosion-deposition rate (SED), MET, and soil nutrient contents (SNs) is closely intertwined. Soil erosion results in a reduction in MET at the top of the slope, while soil deposition increases MET at the slope foot. A notable periodic pattern of SED was observed along the slope (Yu *et al*., 2019; Shen *et al*., 2023). Furthermore, Liu *et al*. (2023) found that within each cycle of varying soil erosion intensity, there were inverse relationships between SED and MET. Soil erosion primarily removes the surface soil, which is the main carrier of soil nutrients and other trace elements (Sun *et al*., 2023). During the erosion process, nutrients are lost, ultimately leading to land degradation. Runoff carries surface soil from higher elevations to lower elevations, altering the spatial distribution of soil particle composition and moisture. This process also impacts the distribution of soil nutrients along the slope (Balasundram *et al*., 2006; Zhang M L *et al*., 2011). Liu *et al*. (2006) found that the spatial distribution of soil nutrients varied with different intensities of soil erosion. Noorbakhsh *et al*. (2008)

*Corresponding author. E-mail: gliu@foxmail.com.

illustrated that there was an increase in SNs from the top to the middle, and further to the bottom of the slope. Soon and Malhi (2005) observed that steep slopes generally contained less soil organic matter (SOM), nitrogen (N), and phosphorus (P) than gentle slopes. Moreover, Lemma *et al*. (2017) documented a yearly decline in SNs, including SOM, total N (TN), and available P (AP), due to soil erosion. However, the main reason for the change in the distribution characteristics of soil nutrients on the slope is that eroded runoff along the slope washes away fine soil particles, which are rich in SOM and various nutrients (Komissarov and Gabbasova, 2017). Soil erosion can cause significant variations in SNs, which consequently impact land productivity and pose a risk to food security (Montanarella *et al*., 2016; Gu *et al*., 2018). Lin *et al*. (2019) found that as soil erosion increased from mild to moderate and severe, the average corn yield decreased by 10.4%–25.4%. The above studies have explored the impact of erosion on SNs and crop yields. Changes in soil thickness caused by SED can significantly affect SNs. Consequently, in areas with thicker soil, it remains unclear whether the impact of SED on nutrients is reduced.

To control soil erosion and mitigate land degradation, various soil and water conservation measures have been developed and applied (Diyabalanage *et al*., 2017; Xu *et al*., 2018). However, the scientific implementation and rational allocation of these measures on tillage slopes still present numerous challenges (Shen *et al*., 2020). In particular, achieving a balance between maximizing soil and water conservation benefits and minimizing land occupation rate is crucial. To address this challenge, it is crucial to accurately understand the relationships among soil erosion, thickness, and nutrients. This knowledge helps identify key positions on slopes for control, such as those with high erosion rates, thin MET, and low SNs.

The objectives of this study were to: i) examine the spatial distribution characteristics of SED, MET, and SNs on slopes and ii) establish correlations among MET, SED, and SNs. The results could contribute to the development of a reliable method for identifying key control positions susceptible to slope erosion and for effectively planning soil and water conservation measures. Furthermore, this study may offer a scientific foundation for enhancing land productivity, increasing grain yield, and evaluating soil erosion and degradation.

MATERIALS AND METHODS

Study area

The study sites were located in Hailun (126°44′45″ E, 47°25′55″ N), Keshan (126°7′59″ E, 48°7′57″ N), and Binxian (127°28′51″ E, 45°52′17″ N) in Heilongjiang, China (Fig. S1, see Supplementary Material for Fig. S1). The predominant landforms at these sites are rolling and hilly plains. Keshan is in the cold temperate zone, while both Binxian and Hailun are situated in the mid-temperate zone. All three sites experience a continental monsoon climate, receiving an annual precipitation of approximately 550 mm on average, with over 80% occurring between May and September. The elevation of the study area ranges from 150 to 470 m. The land use primarily consists of cultivated land, with corn and soybeans being the main crops. The cultivation method is down-slope furrow tillage, with tillage layer depth of 20–25 cm. There are no other soil and water conservation measures on the slopes. According to the USDA soil classification system, the soils in the study area are Mollisols. Selected soil physicochemical properties are listed in Table I.

Experimental design

Due to the significant impact of fertilization levels and management practices on SNs, each selected slope in this study was supplemented with 30–45 t of organic fertilizer per hectare as a basal application, and compound fertilizer was applied to ensure a similar fertility level across all slopes. Ground penetrating radar (GPR) survey lines, five in total, were evenly arranged at intervals according to the slope width, with width ranging from 25 to 33 m. The GPR measurements were conducted along the survey lines, from the slope top to the foot, to acquire a comprehensive image of the MET (A-horizon) on the slope. The data were denoised using RADAN7 software (GSSI, USA), as described by Liu *et al*. (2021). The SED was estimated using the radionuclide ^{137}Cs-tracing technology. Sampling points for ^{137}Cs and soil nutrients were positioned along the survey lines. To ensure representative soil sampling, three soil sample collection strips were arranged at intervals of 50–66 m. According to different slope lengths, soil samples were obtained at 25–30 m intervals using a soil drill (5 cm in diameter). The

TABLE I

Selected physicochemical properties of soils on the slopes at three study sites in Keshan, Binxian, and Hailun, Heilongjiang in the Mollisol region of Northeast China

Site	Clay	Silt	Sand	Bulk density	Organic matter	pH
	%			g cm^{-3}	g kg^{-1}	
Keshan	33.7 ± 2.0	58.6 ± 1.7	7.7 ± 0.6	1.31 ± 0.19	36.2 ± 0.89	6.36 ± 0.12
Binxian	29.8 ± 2.1	60.8 ± 0.9	9.4 ± 1.4	1.39 ± 0.08	27.4 ± 0.77	6.07 ± 0.09
Hailun	31.7 ± 0.8	59.4 ± 1.1	8.9 ± 0.5	1.36 ± 0.02	53.0 ± 2.07	6.27 ± 0.10

sampling depth for ^{137}Cs was 0–30 cm, while the sampling depth for soil nutrients and physicochemical properties was 0–20 cm. A total of 26 sampling locations were evenly distributed on each slope. At each sampling point, soil samples were tested for four types of soil nutrients and ^{137}Cs content. To ensure the accuracy and repeatability of the data, each indicator was measured twice. Therefore, there were a total of 10 soil samples for each sampling point and a total of 260 soil samples for each slope. These samples were used for subsequent soil indicator analyses. The background values of ^{137}Cs at the three research sites were obtained from undisturbed grasslands that had remained unaffected by human activities for more than 70 years (Table II).

TABLE II

Description of basic characteristics[a)] of the slopes at three study sites in Keshan, Binxian, and Hailun, Heilongjiang in the Mollisol region of Northeast China

Characteristic	Keshan	Binxian	Hailun
Slope length (m)	276	200	200
Slope width (m)	120	132	100
Slope gradient (°)	1.72	1.91	1.30
^{137}Cs background value (Bq m^{-2})	2 417	2 379	2 209
Average SED[b)] (t km^{-2} year^{-1})	2 428	2 225	2 160
MET (cm)	22.9	28.6	41.9

[a)] SED = soil erosion-deposition rate; MET = mollic epipedon thickness. [b)] Positive and negative SED values indicate erosion and deposition, respectively.

Sample analysis

Soil samples were air-dried after removing any extraneous materials, such as plant roots and stones, ground, and thoroughly mixed. The ^{137}Cs soil samples were ground and sifted through a 2-mm sieve. Approximately 300 g of soil from each sample was placed into a plastic box for testing. Detailed information on the ^{137}Cs activity test can be found in Liu *et al*. (2023). Following the measurements, the data were interpreted and analyzed to obtain the specific activity of ^{137}Cs.

The soil nutrient samples were meticulously pulverized and sifted through a 0.25-mm sieve to prepare for the assessment of SOM, TN, available potassium (AK), and AP. The determination of SOM was carried out using the external heating method with potassium dichromate (Zhang and Gong, 2012). For TN analysis, the semimicro Kjeldahl method was employed (Hui *et al*., 2023). The AK was extracted by soaking the sample with 0.5 mol L^{-1} ammonium acetate and measured by flame photometry (Li *et al*., 2013). To determine AP, the sample was soaked in 0.5 mol L^{-1} sodium bicarbonate and analyzed using the molybdenum antimony colorimetric method (Zheng, 2005). The measurement was conducted by using a UV-visible spectrophotometer (UV2300, Techcomp Group, China). The particle composition was determined according to Beuselinck *et al*. (1998). Soil bulk density was determined using the cutting ring method. Soil pH value was measured using a portable pH meter (Mettler Toledo, Shanghai).

Data processing and analysis

The SED (t m^{-2} year^{-1}) was calculated based on the simplified mass balance model (Zhang *et al*., 1999) as follows:

$$A = A_0\left(1 - \frac{h}{D}\right)^{n - 1\,963} \tag{1}$$

$$\mathrm{SED} = \rho h \tag{2}$$

where A is the inventory of ^{137}Cs within the soil profile (Bq m^{-2}), n is the sampling year, A_0 is the reference inventory of ^{137}Cs (Bq m^{-2}), h is the depth of annual soil loss (m year^{-1}), D is the depth of the plow layer (m), and ρ is the soil bulk density (g cm^{-3}). Positive and negative SED values indicate erosion and deposition, respectively.

SPSS 26.0 (IBM, USA) software was used for correlation analysis, analysis of variance, and calculation of the root mean square error (RMSE) for MET, SED, and SNs. Data of SED, MET, and SNs from three slopes were used to establish a predictive equation, which was also validated with five sets of data from the top, shoulder, back, foot, and bottom of each slope. The data used for validation and establishment of the equations were mutually independent. Data fitting and the calculation of the coefficient of determination (R^2) were performed using Datafit (Oakdale Engineering, USA). The contour map was drawn using Origin 2023 to describe the distribution characteristics of SED, MET, and SNs on slopes (OriginLab, USA).

RESULTS

Spatial variations in SED and MET

The SED was higher at the top and middle of the slope than at the slope foot (Fig. 1). The SED ranked as follows: Keshan > Hailun > Binxian. The minimum SED on the slope was −950.55 t km^{-2} year^{-1} in Keshan and −54.97 t km^{-2} year^{-1} in Binxian, indicating deposition on the slope (Table III). In Hailun, the minimum SED was 946.22 t km^{-2} year^{-1}, indicating complete erosion without deposition. The variation coefficient for SED was 43% in Keshan and 44% in Binxian, suggesting relatively high variability. In Hailun, the variation coefficient for SED was 26%, indicating intermediate variability.

The variations in MET on the three slopes were similar (Fig. 2). Generally, MET tended to be thinner near the top and back of the slope and thicker at the foot. Moreover, MET displayed wave-like changes along the slope, with variations

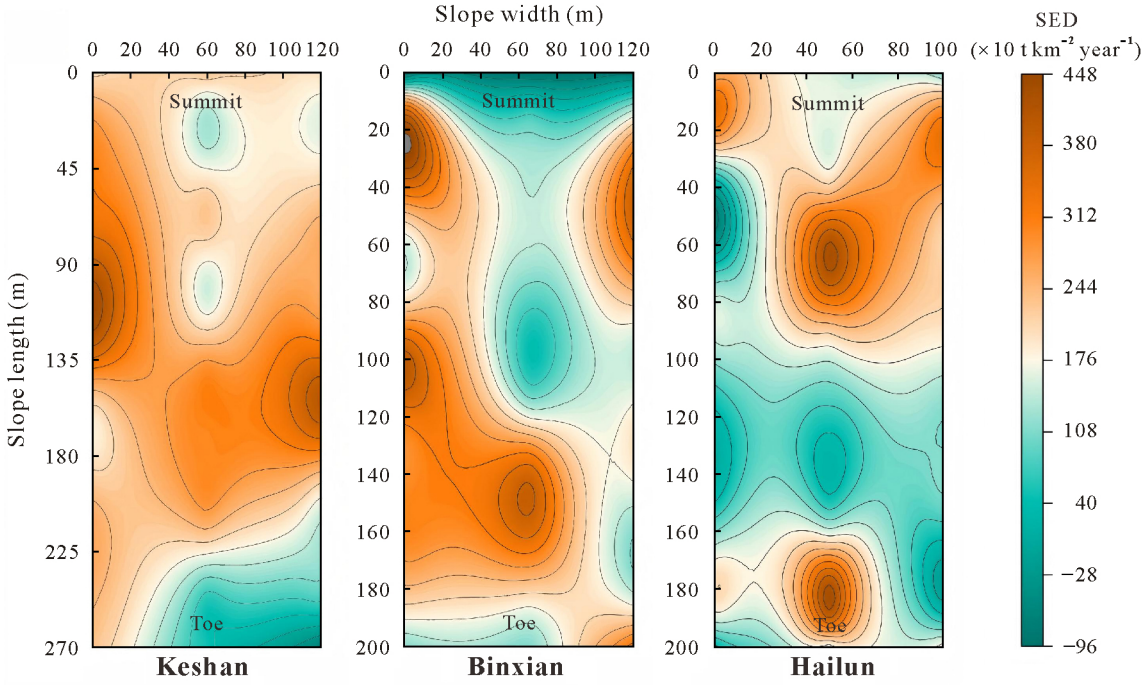

Fig. 1 Spatial distribution of soil erosion-deposition rate (SED) on the slopes at three study sites in Keshan, Binxian, and Hailun, Heilongjiang in the Mollisol region of Northeast China. Positive and negative SED values indicate erosion and deposition, respectively.

TABLE III

Soil erosion-deposition rate (SED) and mollic epipedon thickness (MET) on the slopes at three study sites in Keshan, Binxian, and Hailun, Heilongjiang in the Mollisol region of Northeast China

Site	Parameter	Minimum	Maximum	Mean	Standard deviation	Coefficient of variation
						%
Keshan	SED[a)] (t km^{-2} year^{-1})	−951.0	4 472.0	2 323.0	1 005.0	43.0
	MET (cm)	17.8	27.9	24.2	2.3	90.0
Binxian	SED (t km^{-2} year^{-1})	−55.0	3 142.0	1 787.0	786.0	44.0
	MET (cm)	19.1	36.0	28.0	3.1	11.0
Hailun	SED (t km^{-2} year^{-1})	946.0	3 208.0	2 007.0	526.0	26.0
	MET (cm)	34.2	49.4	43.6	4.1	9.0

[a)] Positive and negative SED values indicate erosion and deposition, respectively.

at different locations. The average MET on the slope in Keshan was 24.17 cm. The MET increased from 23.81 cm within the slope length range of 0–60 m to 25.22 cm within the slope length range of 70–130 m, decreased to 23.36 cm within the slope length range of 135–220 m, and finally increased to 24.66 cm at the slope toe. The average MET on the slope in Binxian was 27.95 cm. Within the slope length range of 60–140 m, the MET on the left side increased, averaging 29.81 cm, while it decreased on the right side, averaging 27.04 cm. Within the slope length range of 150–175 m, MET decreased to 25.22 cm, but then increased again to 28.29 cm within the slope length range at 180 m to the slope toe. The average MET on the slope in Hailun was 43.63 cm. Within the slope length range of 0–60 m, MET was observed to be thinner, with an average value of 40.21 cm. Between the slope lengths of 70–110 m, the middle part of the slope remained thin, with an average MET of 39.25 cm. However, the MET increased on the sides of the slope, with an average value of 45.39 cm. From the slope length at 120 m to the slope toe, MET significantly increased to an average MET of 46.46 cm.

Soil nutrient distribution

The average SOM and TN contents were the highest on the slope in Hailun, with values of 30.2 and 2.41 g kg^{-1}, respectively (Table IV), followed by the slopes in Keshan and Binxian. Additionally, the mean contents of AK and AP were the highest on the slope in Keshan, reaching 214.55 and 47.61 mg kg^{-1}, respectively. The variation coefficient for AP was relatively high on both the Keshan and Binxian slopes, indicating moderate variation. In contrast, the Hailun slope exhibited a high degree of variation.

The changing trends of SOM, TN, AK, and AP along the slope length exhibited a wave-like pattern of increase and

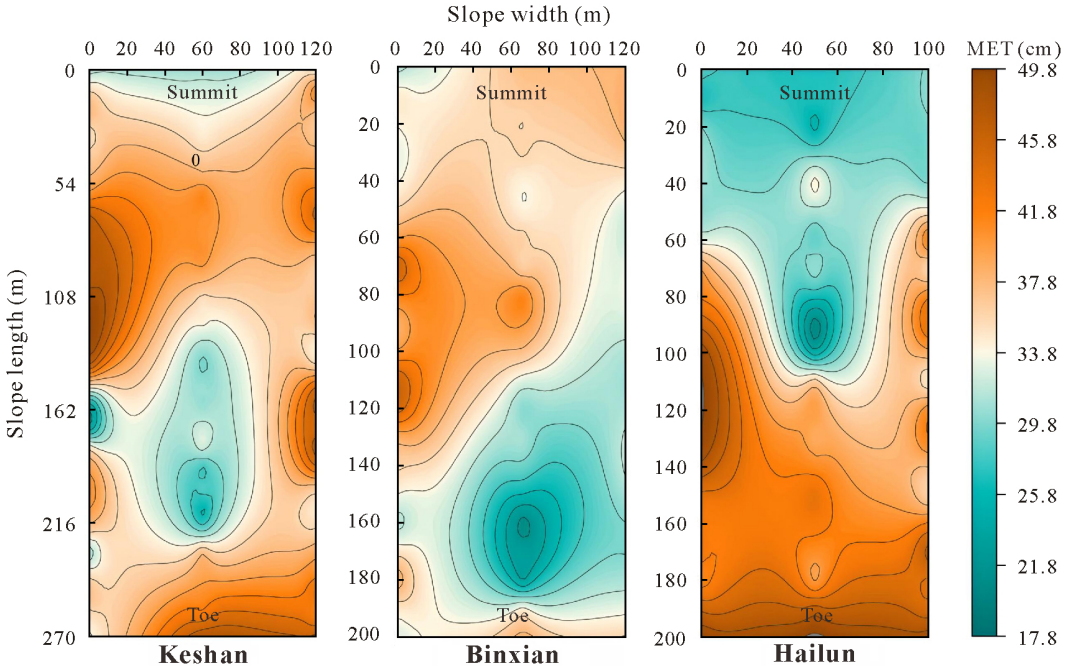

Fig. 2 Spatial variations of the mollic epipedon thickness (MET) on the slopes at three study sites in Keshan, Binxian, and Hailun, Heilongjiang in the Mollisol region of Northeast China.

TABLE IV

Soil nutrient contents (SNs) on the slopes at three study sites in Keshan, Binxian, and Hailun, Heilongjiang in the Mollisol region of Northeast China

Site	SN[a)]	Minimum	Maximum	Mean	Standard deviation	Coefficient of variation
						%
Keshan	SOM (g kg^{-1})	16.1	26.8	20.9	2.6	12.0
	TN (g kg^{-1})	1.4	2.5	1.8	0.2	11.0
	AK (mg kg^{-1})	169.0	285.0	215.0	34.7	16.0
	AP (mg kg^{-1})	18.9	81.1	47.6	12.5	26.0
Binxian	SOM (g kg^{-1})	13.5	24.1	16.2	2.1	13.0
	TN (g kg^{-1})	1.3	1.6	1.4	0.1	4.0
	AK (mg kg^{-1})	99.0	182.0	156.0	13.9	9.0
	AP (mg kg^{-1})	23.5	90.9	50.0	12.9	26.0
Hailun	SOM (g kg^{-1})	20.4	39.5	30.2	3.0	10.0
	TN (g kg^{-1})	2.2	2.6	2.4	0.1	3.0
	AK (mg kg^{-1})	170.0	208.0	184.0	7.8	4.0
	AP (mg kg^{-1})	20.6	147.0	40.5	18.5	46.0

[a)] SOM = soil organic matter; TN = total N; AK = available K; AP = available P.

decrease (Fig. 3). On the slope in Keshan, the SOM and TN contents were notably diminished within the slope length range of 110–200 m compared to other positions along the slope. The contents of AK and AP were high on the right side of the slope and low on the left side. In Binxian, the TN content exhibited a declining trend within the slope length range of 40–120 m. Contrastingly, the other SNs showed an increasing trend along slope length. Moreover, the SNs displayed a downward trend within the slope length range of 120–160 m, but experienced an increasing trend at the slope foot. On the slope in Hailun, there was a significant increase in SNs within the slope length range of 180–200 m. Additionally, the SOM and TN contents were greater on the right side of the slope compared to the left side.

Response of SNs to MET and SED

It was observed that MET was comparatively thinner on the slopes with severe soil erosion, accompanied by a decreasing trend in various SNs (Figs. 1 and 2). To investigate the specific relationship among SNs, MET, and SED, correlation analyses were conducted (Fig. 4). When MET changes by more than 5 cm, it significantly affects SNs and crop yield (Oyedele and Aina, 2006). Therefore, MET was divided into segments at 5-cm intervals. Based on the maximum and minimum values of MET (Table III), the ranges of variation for MET on each slope were determined (Fig. 4). On the slope in Keshan, MET was divided into two ranges: 17.80 cm $\leqslant$ MET $\leqslant$ 22.80 cm and 22.80 cm $<$ MET $\leqslant$ 27.93 cm.

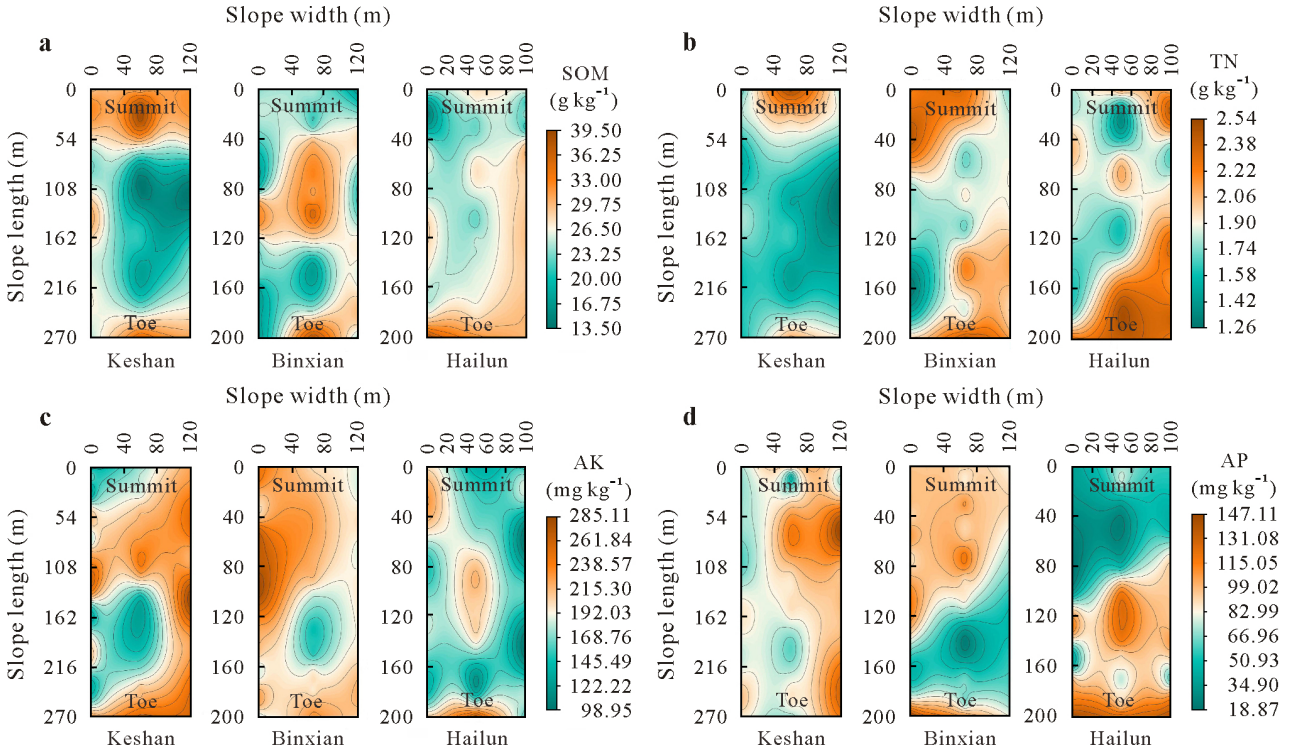

Fig. 3 Spatial distribution of soil organic matter (SOM, a), total N (TN, b), available K (AK, c), and available P (AP, d) on the slopes at three study sites in Keshan, Binxian, and Hailun, Heilongjiang in the Mollisol region of Northeast China.

Similarly, on the slope in Binxian, MET was divided into two ranges: 19.05 cm $\leqslant$ MET $\leqslant$ 29.05 cm and 29.05 cm $<$ MET $\leqslant$ 36.00 cm. On the slope in Hailun, MET was divided into three ranges: 34.24 cm $\leqslant$ MET $\leqslant$ 39.24 cm, 39.24 cm $<$ MET $\leqslant$ 44.24 cm, and 44.24 cm $<$ MET $\leqslant$ 49.38 cm.

A significant negative correlation between SED and MET was observed on each slope (Fig. 4). Specifically, on the slope in Keshan, significant correlations were found among SED, MET, and SNs when MET ranged from 17.8 to 27.93 cm, with the exception of AK. Similarly, on the slope in Binxian, there were also significant correlations among SED, MET, and SNs when MET ranged from 19.05 to 36.00 cm, except for AP for the MET range of 19.05–29.05 cm and AK for the MET range of 29.05–36.00 cm. On the slope in Hailun, as MET increased within the range of 34.24 to 49.38 cm, the correlation between SED and SNs gradually weakened.

In addition, it was observed that when MET surpassed 40 cm, the impact of MET and SED on SNs became insignificant. Hence, for MET less than 40 cm, the regression equation for SNs (SOM (g kg^{-1}), TN (g kg^{-1}), AK (mg kg^{-1}), and AP (mg kg^{-1})) in terms of SED (t km^{-2} year^{-1}) and MET (cm) was established across the three study slopes as follows:

$$\mathrm{SN} = a\mathrm{SED}^{b}\mathrm{MET}^{c} \quad (3)$$

where a, b, and c are constants. A positive numerical value signifies the process of erosion, whereas a negative numerical value signifies the process of deposition. The parameters b and c in Eq. 3 indicated a negative correlation between SNs and SED and a positive correlation between SNs and MET (Table V). This result was consistent with the correlation analysis results (Fig. 4).

Additionally, five sampling locations were selected at various points along the slope, including the top, shoulder, middle, foot, and bottom, to verify the accuracy of the regression equation. These points were independent and not employed in the regression equation. The estimated SNs closely approximated the measured values, with errors in the range of 0.07%–9.77% (Fig. 5).

The threshold for SED was set at 2 500 t km^{-2} year^{-1} (Table VI), which serves as the boundary between moderate and mild erosion in the classification of erosion intensity in the Mollisol region (MWR, 2008). When MET reached or exceeded 40 cm, no significant disparity in SNs was observed, regardless of whether the SED exceeded or remained below 2 500 t km^{-2} year^{-1}. When MET was less than 40 cm, significant disparity was observed in SNs, regardless of whether the SED exceeded or remained below 2 500 t km^{-2} year^{-1}.

DISCUSSION

Soil nutrient distribution along different slopes

The presence of soil nutrients is crucial for crop pro-

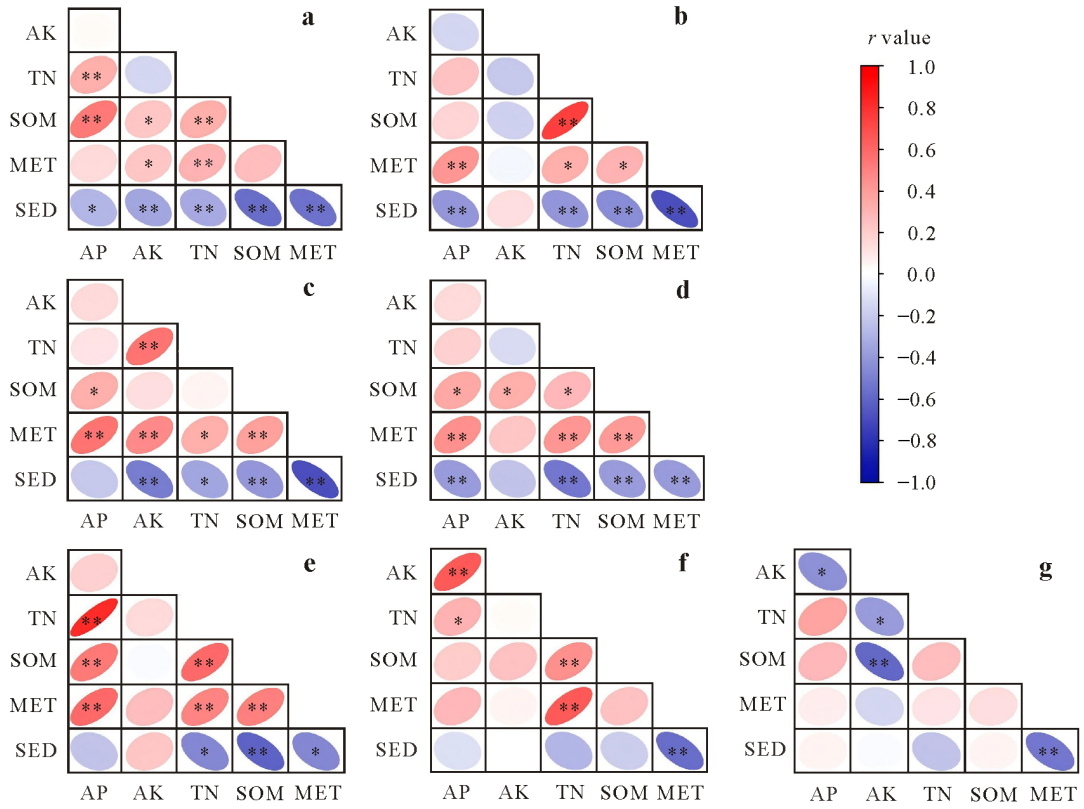

Fig. 4 Relationships among soil erosion-deposition rate (SED), mollic epipedon thickness (MET), and soil nutrient contents (SNs) for different MET ranges on the slopes at three study sites in Keshan, Binxian, and Hailun, Heilongjiang in the Mollisol region of Northeast China: 17.80 cm $\leqslant$ MET $\leqslant$ 22.80 cm (a) and 22.80 cm $<$ MET $\leqslant$ 27.93 cm (b) on the slope in Keshan, 19.05 cm $\leqslant$ MET $\leqslant$ 29.05 cm (c) and 29.05 cm $<$ MET $\leqslant$ 36.00 cm (d) on the slope in Binxian, and 34.24 cm $\leqslant$ MET $\leqslant$ 39.24 cm (e), 39.24 cm $<$ MET $\leqslant$ 44.24 cm (f), and 44.24 cm $<$ MET $\leqslant$ 49.38 cm (g) on the slope in Hailun. Asterisks * and ** indicate significant correlations at $P < 0.05$ and $P < 0.01$, respectively. SOM = soil organic matter; TN = total N; AK = available K; AP = available P.

ductivity, and their spatial distribution is influenced by natural conditions and agricultural management practices (Zhang S L *et al.*, 2011). In our study, sloping farmlands with similar fertilization levels and management modes were selected to minimize the impact of these factors on soil nutrients. Additionally, all three sloping farmlands employed slope ridge cultivation and a corn-soybean rotation system, with corn being the specific crop planted during the sampling year. Furthermore, to minimize the impact of factors other than SED and MET on SNs, three selected slopes had identical terrain characteristics, consisting of straight slopes with minimal variation in the slope gradient.

However, it should be noted that there were variations in the average annual rainfall across the three study sites (Fig. S1). This difference in rainfall may account for the variations observed in SNs among the different study sites. Rainfall typically has a positive impact on soil nutrient storage. The increase in rainfall promotes the growth of vegetation biomass and enhances the contents of carbon (C) and N in soil through the input of organic matter (Lin *et al.*, 2012). Based on the comparison of SNs across different study sites (Table IV), it was evident that the SOM and TN contents were notably higher in Hailun than those at the other two sites,

TABLE V

Parameters[a)] of the regression equation for soil nutrient contents (SNs) in terms of soil erosion-deposition rate and mollic epipedon thickness on the slopes at three study sites in Keshan, Binxian, and Hailun, Heilongjiang in the Mollisol region of Northeast China

Site	SN[b)]	a	b	c	R^2	RMSE
						g kg^{-1} or mg kg^{-1}[c)]
Keshan	SOM	7.72	−0.08	0.50	0.63	1.18
	TN	1.49	−0.10	0.29	0.64	0.09
	AK	477	−0.11	0.01	0.52	9.32
	AP	11.7	−0.07	0.61	0.58	3.43
Binxian	SOM	15.4	−0.10	0.24	0.66	0.69
	TN	1.16	−0.01	0.09	0.67	0.02
	AK	130	−0.02	0.09	0.60	2.22
	AP	9.66	−0.13	0.77	0.53	5.74
Hailun	SOM	21.6	−0.08	0.27	0.60	0.63
	TN	1.86	−0.07	0.23	0.59	0.04
	AK	91.6	−0.002	0.20	0.53	1.53
	AP	0.01	−0.08	2.91	0.63	13.1

[a)] a, b, and c are constants; RMSE is the root mean square error.
[b)] SOM = soil organic matter; TN = total N; AK = available K; AP = available P.
[c)] g kg^{-1} for the RMSE of the regression equation for SOM and TN; mg kg^{-1} for the RMSE of the regression equation for AK and AP.

even though the entire slope underwent complete erosion without deposition. This disparity may be attributed to the

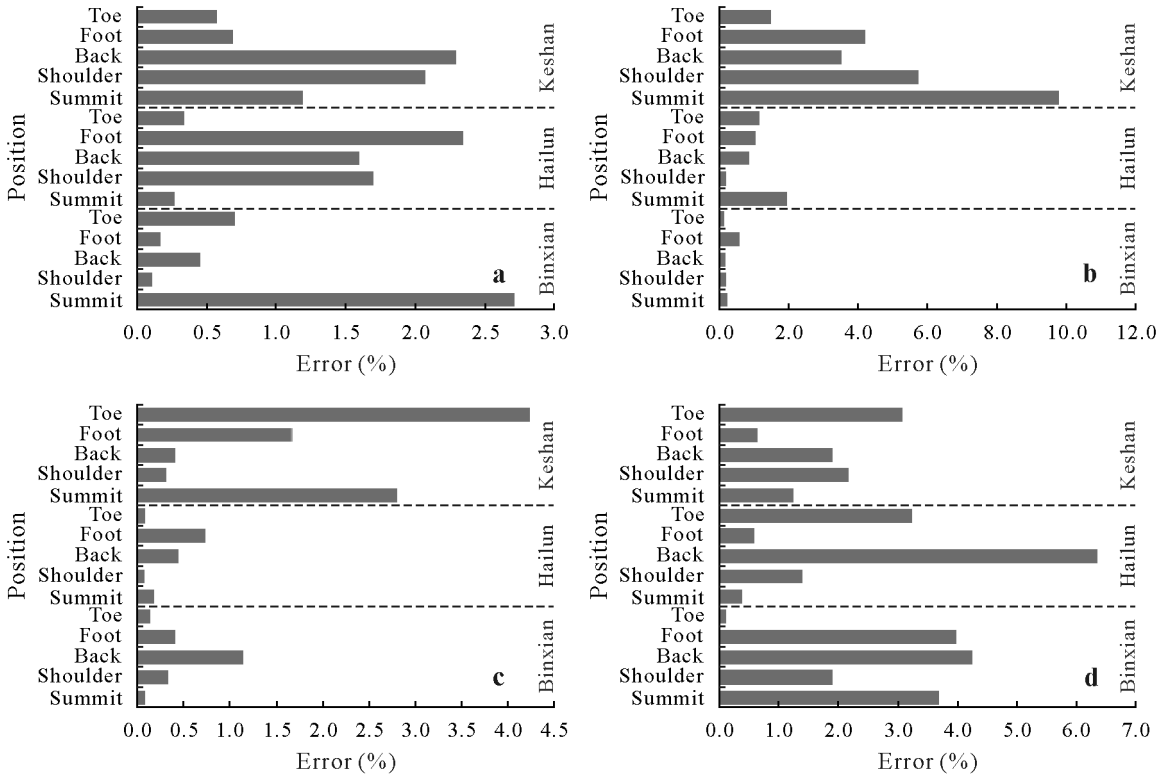

Fig. 5 Errors between measured and predicted soil organic matter (a), total N (b), available K (c), and available P (d) contents at different positions on the slopes at three study sites in Keshan, Binxian, and Hailun, Heilongjiang in the Mollisol region of Northeast China.

TABLE VI

Soil nutrient contents (SNs) on the slopes with different mollic epipedon thicknesses (MET) and soil erosion-deposition rates (SEDs) at three study sites in Keshan, Binxian, and Hailun, Heilongjiang in the Mollisol region of Northeast China

Site	SN[a)]	SED[b)]	
		$< 2\,500$ t km^{-2} year^{-1}	$\geqslant 2\,500$ t km^{-2} year^{-1}
		MET $\geqslant 40$ cm	
Hailun	SOM (g kg^{-1})	30.46a[c)]	29.98a
	TN (g kg^{-1})	2.41a	2.43a
	AK (mg kg^{-1})	183.24a	184.81a
	AP (mg kg^{-1})	38.30a	39.98a
		MET < 40 cm	
Keshan	SOM (g kg^{-1})	21.63a	19.85b
	TN (g kg^{-1})	1.81a	1.67b
	AK (mg kg^{-1})	219.46a	208.14b
	AP (mg kg^{-1})	50.47a	44.54b
Binxian	SOM (g kg^{-1})	16.33a	15.60b
	TN (g kg^{-1})	1.42a	1.38b
	AK (mg kg^{-1})	156.81a	151.11b
	AP (mg kg^{-1})	51.38a	44.75b
Hailun	SOM (g kg^{-1})	30.29a	27.46b
	TN (g kg^{-1})	2.36a	2.41b
	AK (mg kg^{-1})	184.00a	191.14b
	AP (mg kg^{-1})	63.34a	37.49b

[a)] SOM = soil organic matter; TN = total N; AK = available K; AP = available P.

[b)] The SED threshold of 2 500 t km^{-2} year^{-1} was set according to MWR (2008) to classify the slope soil erosion intensity into mild (SED $< 2\,500$ t km^{-2} year^{-1}) and moderate (SED $\geqslant 2\,500$ t km^{-2} year^{-1}) erosion.

[c)] Means followed by different letters in the same row are significantly different at $P < 0.05$.

higher annual precipitation in Hailun, resulting in greater soil moisture content and a reduced rate of SOM decomposition, consequently sustaining higher SNs (Huang, 2000). At the same time, the intensive rainfall is also an important factor affecting the loss of soil nutrients. Short bursts of heavy rainfall may lead to significant soil erosion, and water and soil carry away a large amount of nutrients (Durán Zuazo *et al*., 2004). Under different rainfall intensities, cumulative runoff, nutrient loss, and sediment transport all increase as a power function of increasing rainfall intensity (Hao *et al*., 2015). As the soil erosion intensity increases, the contents of SOM, TN, and AP always decrease, aligning with the erosion type and intensity (Zhang M L *et al*., 2011). The enrichment of SOM and TN on the soil surface makes them susceptible to the movement of surface soil (Nadeu *et al*., 2012; Nie *et al*., 2018).

Interactions among SED, MET, and SNs

The positions with higher SED exhibited a thin layer of MET, and the changes in both SED and MET on the slope were characterized by a wave-like pattern of alternating increases and decreases. Soil erosion also affects soil physicochemical properties, SOM, and SNs (Borrelli *et al*., 2018; Gu *et al*., 2018). Conversely, soil physicochemical properties, along with soil quality, can also contribute to the intensification of soil erosion. Soil erosion transports

organic C-rich soil particles to sedimentary areas, resulting in lower organic C content in severely eroded areas (Osman, 2014; Sarapatka *et al*., 2018; Zhao *et al*., 2018). Wang *et al*. (2009) found that under conventional fertilization conditions, soybean yield showed an exponential decline with increasing soil erosion depth. On average, there was a 14.9% reduction in yield for every 10 cm of soil erosion. This could be attributed to the loss of SOM, N, and P. The slope foot within the slope length range of 160–200 m in Hailun experienced a high SED. However, nutrient-rich fine particles from severely degraded areas, such as hilltops and backslopes, were deposited at the slope toe, leading to the development of thicker Mollisol layers and an augmentation in SNs. No significant correlation between SED and SNs was found when MET was high ($>$ 40 cm) (Fig. 4). The impact of MET on SNs was more significant than SED in Hailun. This could be attributed to the presence of a thick original MET, which mitigated the effect of SED on SNs. However, in Keshan, where the MET was thin, the influence of SED on SNs exceeded that of MET. Therefore, the role of MET in affecting SNs should not be overlooked.

Determination of the priority position of erosion control

To control severe soil erosion in the Mollisol region in Northeast China, extensive soil and water conservation measures, such as contour tillage, no-tillage, terraces, and hedgerows, have been actively employed since 2000 (Fang, 2021). No-till technology can effectively improve the stability of soil aggregates and enhance soil quality (Komissarov and Klik, 2020). Zhang *et al*. (2021) found that for all damaged, high-hazard, and moderate-hazard farmlands, no-till is the best practice. Furthermore, if the best soil and water conservation measures are implemented immediately, 82% of sloping farmlands can maintain an A-horizon thicker than 20 cm. Due to the requirements of certain accumulated temperature conditions, no-till measures are applicable to the fourth and fifth accumulated temperature zones in Heilongjiang Province, but are difficult to fully apply in areas with lower accumulated temperatures (Dai *et al*., 2023). Jia *et al*. (2022) reported that terraced fields demonstrate favorable soil and water conservation benefits, even under extreme rainfall conditions, with SED reduced by 67.67% and 78.63% in two small watersheds. Hu *et al*. (2022) revealed that the application of soil and water conservation measures in small watersheds led to an annual increase of 0.33% in surface SOM. However, the selection, allocation, and combination of different measures can affect the efficiency of soil erosion control (Xu *et al*., 2018; Li *et al*., 2021). Previous studies predominantly focused on the impact of soil and water conservation measures on SED or SNs, often neglecting the effects of the depth of the effective soil layer or soil tillage layer. Therefore, based on the findings of our study, it is recommended to comprehensively consider SNs, SED, and MET to control soil erosion (Table VI). In consideration of the distribution of MET, SED, and SNs on the slope, priority areas for controlling soil erosion on the slope were determined. Appropriate soil and water conservation measures were then recommended for these areas. When MET reached or exceeded 40 cm, it is advisable to prioritize areas with thinner MET or higher erosion rates for the implementation of soil and water conservation measures to mitigate surface soil loss and preserve soil layer thickness. When MET was less than 40 cm, it is recommended that efforts primarily focus on reducing SED as a vital management task to prevent the reduction of soil thickness. This approach should particularly target areas with lower SNs to prevent significant impact of nutrient loss on crop yields.

Furthermore, the results of our study can be extrapolated to the watershed scale. Fang (2021) found that soil erosion within a basin could be effectively managed through the implementation of appropriate soil and water conservation measures. The results demonstrated the efficacy of employing specific conservation practices based on the slope characteristics of small watersheds. For instance, contour tillage was applied on slopes below 3°, and terraces were constructed on 5°–8° slopes. However, it is important to note that when planning soil and water conservation measures in a watershed, the distribution characteristics of MET, SED, and SNs on slopes should be fully considered for each up-, mid-, and downstream position. In addition, our study had some limitations. The distribution of soil nutrients on slopes is influenced by numerous factors, including gradient, aspect, and farming methods. Further investigation of these additional variables is necessary.

CONCLUSIONS

At the study sites in Keshan, Binxian, and Hailun, SED exhibited moderate variation and an uneven distribution across the slope. The SED was higher at the top and middle of the slope and lower at the foot. There was an inverse spatial distribution trend between SED and MET. The MET and SED exhibited a wave-like changing trend along the slope. The spatial distributions of SOM, TN, AK, and AP were influenced by both SED and MET, resulting in an uneven pattern with wave-like fluctuations along the slope. Typically, SNs tended to be lower toward the back of the slope and higher near the slope foot, with an increase with increasing MET. Correlation analysis results indicated an inverse relationship between MET and SED—a negative correlation between SNs and SED and a positive correlation between MET and SNs. Notably, when MET exceeded 40 cm, there was a decreased negative correlation between SED and SNs. Furthermore, a robust regression equation was established for MET, SNs, and SED, further confirming their interconnectedness. The

error range of the fitted equation was between 0.07% and 9.77%. These findings highlighted the intricate interactions among SED, MET, and SNs. When designing soil and water conservation measures, it is necessary to comprehensively consider SED, MET, and SNs at different positions on the slopes. The results provide a novel perspective for identifying the priority position of slope erosion control and serve as a crucial scientific foundation for assessing soil erosion degradation.

DECLARATION OF COMPETING INTEREST

The authors declare that they have no known competing financial interests or personal relationships that could have appeared to influence the work reported in this paper.

ACKNOWLEDGEMENT

This research was supported by the Strategic Priority Research Program of Chinese Academy of Sciences (No. XDA28010201).

SUPPLEMENTARY MATERIAL

Supplementary material for this article can be found in the online version.

REFERENCES

Adimassu Z, Mekonnen K, Yirga C, Kessler A. 2014. Effect of soil bunds on runoff, soil and nutrient losses, and crop yield in the Central Highlands of Ethiopia. *Land Degrad Dev*. **25**: 554–564.

Balasundram S K, Robert P C, Mulla D J, Allan D L. 2006. Relationship between oil palm yield and soil fertility as affected by topography in an Indonesian plantation. *Commun Soil Sci Plant Anal*. **37**: 1321–1337.

Beuselinck L, Govers G, Poesen J, Degraer G, Froyen L. 1998. Grain-size analysis by laser diffractometry: Comparison with the sieve-pipette method. *Catena*. **32**: 193–208.

Borrelli P, Van Oost K, Meusburger K, Alewell C, Lugato E, Panagos P. 2018. A step towards a holistic assessment of soil degradation in Europe: Coupling on-site erosion with sediment transfer and carbon fluxes. *Environ Res*. **161**: 291–298.

Dai Y J, Liu Y F, Wang Y L, Fang W Y, Chen Y M, Sui Y Y. 2023. A practice of conservation tillage in the Mollisol region in Heilongjiang Province of China: A mini review. *Pol J Environ Stud*. **32**: 1479–1489.

Diyabalanage S, Samarakoon K K, Adikari S B, Hewawasam T. 2017. Impact of soil and water conservation measures on soil erosion rate and sediment yields in a tropical watershed in the Central Highlands of Sri Lanka. *Appl Geogr*. **79**: 103–114.

Durán Zuazo V H, Martínez Raya A, Aguilar Ruiz J. 2004. Nutrient losses by runoff and sediment from the taluses of orchard terraces. *Water Air Soil Pollut*. **153**: 355–373.

Fang H Y. 2021. Using WaTEM/SEDEM to configure catchment soil conservation measures for the black soil region, northeastern China. *Sustainability*. **13**: 10421.

Feng Z Z, Zheng F L, Hu W, Li G F, Xu X M. 2018. Impacts of mollic epipedon thickness and overloaded sediment deposition on corn yield in the Chinese Mollisol region. *Agric Ecosyst Environ*. **257**: 175–182.

Gu Z J, Xie Y, Gao Y, Ren X Y, Cheng C C, Wang S C. 2018. Quantitative assessment of soil productivity and predicted impacts of water erosion in the black soil region of northeastern China. *Sci Total Environ*. **637-638**: 706–716.

Hao C L, Yan D H, Xiao W H, Shi M, He D W, Sun Z X. 2015. Impacts of typical rainfall processes on nitrogen in typical rainfield of black soil region in Northeast China. *Arab J Geosci*. **8**: 6745–6757.

Hu W, Xu J Z, Li J Y, Zhang X Y. 2022. The effect of soil and water conservation measures on soil organic carbon in a typical small watershed in the Mollisol region of Northeast China. *Catena*. **208**: 105744.

Huang C Y. 2000. Soil Science (in Chinese). China Agriculture Press, Beijing.

Hui R, Tan H J, Li X R, Zhao R M, Yang H T. 2023. A comparative study of soil nutrient availability and enzyme activity under biological soil crusts in different erosion regions of the Loess Plateau, China. *Plant Soil*. **484**: 425–440.

Institute of Geographic Sciences and Natural Resources Research, Chinese Academy of Sciences (IGSNRR CAS). 2023. Report on the protection and utilization of the black soil in Northeast China (in Chinese). Available online at https://finance.sina.com.cn/tech/roll/2025-03-24/doc-ineqsqya8352449.shtml (verified on January 16, 2024).

Jia H, Wang X D, Sun W Y, Mu X M, Gao P, Zhao G J, Li Z X. 2022. Estimation of soil erosion and evaluation of soil and water conservation benefit in terraces under extreme precipitation. *Water*. **14**: 1675.

Komissarov M A, Gabbasova I M. 2017. Erosion of agrochernozems under sprinkler irrigation and rainfall simulation in the southern forest-steppe of Bashkir Cis-Ural region. *Eurasian Soil Sci*. **50**: 253–261.

Komissarov M A, Klik A. 2020. The impact of no-till, conservation, and conventional tillage systems on erosion and soil properties in Lower Austria. *Eurasian Soil Sci*. **53**: 503–511.

Lemma B, Kebede F, Mesfin S, Fitiwy I, Abraha Z, Norgrove L. 2017. Quantifying annual soil and nutrient lost by rill erosion in continuously used semiarid farmlands, North Ethiopia. *Environ Earth Sci*. **76**: 190.

Li F L, Liu M, Li Z P, Jiang C Y, Han F X, Che Y P. 2013. Changes in soil microbial biomass and functional diversity with a nitrogen gradient in soil columns. *Appl Soil Ecol*. **64**: 1–6.

Li H L, Shen H O, Wang Y, Wang Y, Gao Q. 2021. Effects of ridge tillage and straw returning on runoff and soil loss under simulated rainfall in the Mollisol region of Northeast China. *Sustainability*. **13**: 10614.

Lin C, Zhou S L, Wu S H, Liao F Q. 2012. Relationships between intensity gradation and evolution of soil erosion: A case study of Changting in Fujian Province, China. *Pedosphere*. **22**: 243–253.

Lin H H, Xie Y, Liu G, Zhai J R, Li S. 2019. Soybean and maize simulation under different degrees of soil erosion. *Field Crops Res*. **230**: 1–10.

Liu C, Liu G, Dan C X, Shen E S, Li H R, Zhang Q, Guo Z, Zhang Y. 2023. Variability in mollic epipedon thickness in response to soil erosion-deposition rates along slopes in Northeast China. *Soil Tillage Res*. **227**: 105616.

Liu C, Liu G, Li H R, Wang X K, Chen H, Dan C X, Shen E S, Shu C B. 2021. Using ground-penetrating radar to investigate the thickness of mollic epipedons developed from loessial parent material. *Soil Tillage Res*. **212**: 105047.

Liu D W, Wang Z M, Zhang B, Song K S, Li X Y, Li J P, Li F, Duan H T. 2006. Spatial distribution of soil organic carbon and analysis of related factors in croplands of the black soil region, Northeast China. *Agric Ecosyst Environ*. **113**: 73–81.

Liu K, Wei M H, Dai H M, Liu G D, Jia S H, Song Y H, Liang S. 2022. Spatiotemporal variation of black soil layer thickness in black soil region of Northeast China. *Geol Res* (in Chinese). **31**: 434–442, 394.

Liu X B, Zhang S L, Zhang X Y, Ding G W, Cruse R M. 2011. Soil erosion control practices in Northeast China: A mini-review. *Soil Tillage Res*. **117**: 44–48.

Ministry of Water Resources of the People's Republic of China (MWR). 2008. Standards for Classification and Gradation of Soil Erosion (SL 190–2007) (in Chinese). China Water & Power Press, Beijing.

Montanarella L, Pennock D J, McKenzie N, Badraoui M, Chude V, Baptista I, Mamo T, Yemefack M, Singh Aulakh M, Yagi K, Young Hong S, Vijarnsorn P, Zhang G L, Arrouays D, Black H, Krasilnikov P, Sobocká J, Alegre J, Henriquez C R, de Lourdes Mendonça-Santos M, Taboada M, Espinosa-Victoria D, Alshankiti A, Alavipanah S K, Elsheikh E A

E M, Hempel J, Camps Arbestain M, Nachtergaele F, Vargas R. 2016. World's soils are under threat. *Soil*. **2**: 79–82.

Nadeu E, Berhe A A, de Vente J, Boix-Fayos C. 2012. Erosion, deposition and replacement of soil organic carbon in Mediterranean catchments: A geomorphological, isotopic and land use change approach. *Biogeosciences*. **9**: 1099–1111.

Nie X D, Li Z W, Huang J Q, Liu L, Xiao H B, Liu C, Zeng G M. 2018. Thermal stability of organic carbon in soil aggregates as affected by soil erosion and deposition. *Soil Tillage Res*. **175**: 82–90.

Noorbakhsh S, Schoenau J, Si B, Zeleke T, Qian P. 2008. Soil properties, yield, and landscape relationships in South-Central Saskatchewan Canada. *J Plant Nutr*. **31**: 539–556.

Osman K T. 2014. Soil Degradation, Conservation and Remediation. Springer, Dordrecht.

Oyedele D J, Aina P O. 2006. Response of soil properties and maize yield to simulated erosion by artificial topsoil removal. *Plant Soil*. **284**: 375–384.

Sarapatka B, Cap L, Bila P. 2018. The varying effect of water erosion on chemical and biochemical soil properties in different parts of Chernozem slopes. *Geoderma*. **314**: 20–26.

Shen H O, Wang D L, Wen L L, Zhao W T, Zhang Y. 2020. Soil erosion and typical soil and water conservation measures on hillslopes in the Chinese Mollisol region. *Eurasian Soil Sci*. **53**: 1509–1519.

Shen Y L, Gu J, Liu G, Wang X K, Shi H Q, Shu C B, Zhang Q, Guo Z, Zhang Y. 2023. Predicting soil erosion and deposition on sloping farmland with different shapes in Northeast China by using ^{137}Cs. *Catena*. **229**: 107238.

Soon Y K, Malhi S S. 2005. Soil nitrogen dynamics as affected by landscape position and nitrogen fertilizer. *Can J Soil Sci*. **85**: 579–587.

Sun W X, Niu X Y, Wang Y P, Yin X W, Teng H W, Gao P L, Liu A J. 2023. Effects of forest age on soil erosion and nutrient loss in Dianchi watershed, China. *Environ Monit Assess*. **195**: 340.

Wang Z Q, Liu B Y, Wang X Y, Gao X F, Liu G. 2009. Erosion effect on the productivity of black soil in Northeast China. *Sci China Ser D: Earth Sci*. **52**: 1005–1021.

Xu X M, Zheng F L, Wilson G V, He C, Lu J, Bian F. 2018. Comparison of runoff and soil loss in different tillage systems in the Mollisol region of Northeast China. *Soil Tillage Res*. **177**: 1–11.

Yu Y, Zhang K L, Liu L, Ma Q H, Luo J Y. 2019. Estimating long-term erosion and sedimentation rate on farmland using magnetic susceptibility in Northeast China. *Soil Tillage Res*. **187**: 41–49.

Zhang F. 2020. Current situation and control model of eroded gully in black soil area of Northeast China. *Soil Water Conserv China* (in Chinese). **12**: 54–55, 79.

Zhang G L, Gong Z T. 2012. Soil Survey Laboratory Methods (in Chinese). Science Press, Beijing.

Zhang M L, Yang H, Zou J, Xu L J, Sui Z L. 2011. Effects of soil erosion on soil quality in the rocky mountain areas of northern China. *J Soil Water Conserv* (in Chinese). **25**: 218–221.

Zhang S L, Zhang X Y, Huffman T, Liu X B, Yang J Y. 2011. Influence of topography and land management on soil nutrients variability in Northeast China. *Nutr Cycl Agroecosyst*. **89**: 427–438.

Zhang T Y, Wilson G V, Hao Y F, Han X. 2021. Erosion hazard evaluation for soil conservation planning that sustains life expectancy of the A-horizon: The black soil region of China. *Land Degrad Dev*. **32**: 2629–2641.

Zhang X B, Walling D E, He Q. 1999. Simplified mass balance models for assessing soil erosion rates on cultivated land using caesium-137 measurements. *Hydrol Sci J*. **44**: 33–45.

Zhang Y G, Wu Y Q, Liu B Y, Zheng Q H, Yin J Y. 2007. Characteristics and factors controlling the development of ephemeral gullies in cultivated catchments of black soil region, Northeast China. *Soil Tillage Res*. **96**: 28–41.

Zhao P Z, Li S, Wang E H, Chen X W, Deng J F, Zhao Y S. 2018. Tillage erosion and its effect on spatial variations of soil organic carbon in the black soil region of China. *Soil Tillage Res*. **178**: 72–81.

Zheng F L. 2005. Effects of accelerated soil erosion on soil nutrient loss after deforestation on the Loess Plateau. *Pedosphere*. **15**: 707–715.